Cement Water Treatment Process Hybrid Bond Graph Modeling and Robust Diagnosis

Eya Fathallah and Nadia Zanzouri

National Engineering School of Tunis Laboratory ACS Department of Electrical Engineering Box 37,1002 Tunis Belvedere

Summary
This paper proposes firstly an Hybrid Bond Graph modelling of the cement water treatment process. Then, it treats the issue of the mode identification for the hybrid dynamic systems in the presence of the uncertainties of measurements both in healthy and faulty cases. It presents a graphical approach dedicated to the hybrid bond graph domain. An hybrid observer is constructed based on BG-LFT model suitable simultaneously to identify the current mode and to detect and locate the sensor fault. In fact, this complex process contains different components presenting a diversity of physical phenomena which leads to the interaction between several domains such as hydraulic, chemical, electrical, mechanical, etc. Usually, the industrial systems are considered as systems with hybrid dynamic which increases the degrees of difficulty of the modeling process. To overcome these constraints, an efficient tool of modeling is needed so the choice of using an hybrid bond graph to model this process. An experimental characterization of the system is performed in order to assess the validated bond graph model of the studied process. Finally, the simulation results obtained from this elaborated model reveal a significant conformity compared to the experimental results and demonstrate the efficiency of the hybrid bond graph approach.

.Key words:
Hybrid bond graph modeling; Cement water treatment; Experimental characterization; mode identification; measurements uncertainties.

1. Introduction

The water treatment system is a sophisticated system playing a primordial role in the functioning of many processes especially in the heavy industry such as cement plant. It is considered as complicated system because it contains a large number of components and is the result of many interacting domains such as hydraulic, electrical, mechanical and chemical domains. Such system diversity of integrating several kinds of energy behavior makes the modeling process of these multidisciplinary systems difficult due to the fact that the most current software tools can only operate in a single domain. Hence, the Hybrid Bond Graph (HBG) formalism can be seen as powerful tool that is well adapted for dynamic modeling of such a multi-physical system [1]. Nowadays, the modeling community is interested in the hybrid dynamic system (HDS) thanks to its ability to represent the industrial systems in a more real way than any other dynamics. The major advantage of this dynamic is that it combines in one way or another, the dynamic of the continuous parts of the system with the dynamic of the logic and discrete parts. In the latter of 1990s, many suggestions of modeling the (HDS) were presented in the literature. The most interesting of these is the hybrid bond graph. The bond graph is a well-known multidisciplinary tool suitable for many engineering domains. Indeed, the topic of modeling discontinuities in bond graph is currently an active domain of research. In reality, researchers classify the hybrid bond graph models into two categories. The first one is called the fixed causality approach where the switching elements preserve the causality of these systems and only the varying parameters at the switching instants. Many models were developed to express this technique. For example, the model in [2] uses the modulated resistor as a switching element. It accords an important value to the resistor to express the ON state then it decreases this value to have the OFF state. Another model is proposed by [3] where the switching element is represented by combining a transformer, which commands the switching process, with a fixed resistor. In a similar vein, the authors in [4] propose the modulated transformer. Later in [5], the model develops bonds modulated by a zero or one signal. When the signal is zero, the bond must disappear; and when it is one, the system considers the presence of this bond. This approach is more developed in [6].The second category of the hybrid bond graph model focuses on systems where their causalities vary after switching. Many works has dealt with this topic such as the switched source where the switch is modeled as a source of commutation between the source of the null flow and the null effort, imposing a zero flow/effort at the connecting junction when OFF [7]. Based on the switched source, the authors in [8] present the switched storage element as a compound element, acting as a regular storage element when ON and a switched source (null source) when OFF. Shortly afterwards, the work in [9] presented the controlled junction which is a regular 0- or 1- junction when ON and a null source on each bond when OFF.
The hybrid dynamic system remains a fertile domain of research, it englobes many subjects to be carefully treated.

Manuscript received March 5, 2017
Manuscript revised March 20, 2017

A one of these is the method of mode identification which plays an important role in the hybrid system diagnosis. Among the literature, the procedures of the mode identification of the HDS are numerous and different. A part of them are based on the use of the observers as recalled in [10], [11] and [12]. Others techniques derived from the analytical redundancy relations (ARRs) are based on the residuals consistency as stated in [13] and [14]. The topic of the mode identification also interests the bond graph community. Then for the hybrid bond graph, this issue is elaborated by many authors. To state, [15] shows that ARR residuals derived from a bond graph cannot only serve as fault indicators but may also be used for bond graph model based system mode identification. Another recent approach starts from a bond graph with controlled junctions, in whom computational causalities are mode dependent, and proposes to derive a power relation from the bond graph for each system mode [16]. After, [17] evoke a mode identification method for hybrid systems in the presence of fault. The method is presented as a module of an HBG-based quantitative health monitoring framework. This framework utilizes the concept of GARRs and integrates several steps and modules.

The robust diagnosis becomes nowadays an important domain of research in recent years, especially for the works including a real application. For the bond graph domain, several robust methods of fault detection and isolation (RFDI) have been proposed in the literature such as in [18] and [19].

This paper presents in addition to the modelling of the real process of water treatment of the Djebel Ressas's cement plant, a mode identification approach basing on different methods of residuals evaluation; citing the graphical method of evaluation basing on bond graph and also the norm method focusing in assessing the quadratic average residuals. Accordingly, the first section includes a detailed description of the cement water treatment process. In section 2, a hybrid bond graph model of whole system is proposed with the aim of imitating the real behavior of the system. Section 3 is dedicated to the experimental background of this system which is then compared to the simulation results developed from the model. Section 4 explains the procedure of the mode identification in the presence of measurement uncertainties in healthy and faulty case. Section 5 presents the efficiency of this approach applied to the simplified cement water treatment process. The final section presents the conclusion.

2. Cement Water Treatment Process Modeling

2.1 The description of the process

Fig. 1. The cement water treatment process.

The cement water treatment system consists of two parallel treatment trains together with an installed sand filtration and reverses osmosis (RO) demineralization. After the step of the RO demineralization, some raw water can be blended with the dosing of the sodium hydroxide. A dosing of an inhibitor chemical is done to makeup a water feed line to cool the water circuit. A small partial stream of the demineralized water obtained after the reverse osmosis can be treated to produce potable water. In this study, the raw water treatment is done to supply water to the circuit of the cooling water. The cement water treatment system consists of several equipment performing interdependent unit operations. The water treatment process is a sequence of operations required to reach the anticipated quality. The functioning of the equipment is briefly described in the following section. The raw water tank (761.TK100) is the storage of the incoming raw water from the source. During the treatment process, the water flow is pumped with two raw water pumps (761.WP110 &761.WP111). During the normal operation, only one raw water pump is running and is able to feed both filters (761.FU120 and 761.FU121) with a total flow of 72 m3/hour. Each of the two parallel filters (known as sand filters) feeds one reverse osmosis unit. The capacity of each filter is 36 m3/hour and is fed by the raw water pumps. This sand filtration operation removes the suspended solids and particles from the raw water which can deteriorate the performance of the reverse osmosis membranes. Pressure filters are also intended to protect the subsequent RO process during abrupt situations when the best water quality changes. After that, the two parallel reverse osmosis units (line 1 and 2) are installed. The reverse osmosis is the finest filtration used to purify water and remove salts and other impurities in order to improve the properties of the water. The reverse osmosis uses a semi- permeable membrane allowing the water to

pass through while rejecting the remaining contaminants. The process of the reverse osmosis requires a driving force to push the pure water through the membrane, typically a high pressure pump. All water cannot be filtered through the membrane; hence the need for the reject of about 25 – 50 % of feed flow. One reverse osmosis unit is able to produce 25 m3/hour of demineralized water called permeate. If raw water salinity increases to "maximum", the permeate flow will become lower due to the increased osmotic pressure of the concentrate. The capacity of one reverse osmosis unit at "maximum" raw water parameters is 21 (m3/hour), while the total capacity is 42 (m3/hour).
As for the water distribution system, the raw water system supplies water to the cooling water tank (762TK100) which is subdivided into a cold tank and a hot tank when the level indicators (762.TK100N01&762.TK100N01) in the cooling water tank indicate a low level. In fact, this level governs the functioning of the RO and the raw water treatment in the following way: when the level of the cooling water reservoir lowers, it will give a "run signal" to the raw water treatment process. The tank level shall determine if one or two RO units are operating. Several levels can be set to the reservoir as follows:
Low level 1< 2.5 m: Start one RO unit.
Low level 2= 2.50 m: Start both RO units.
High level 1= 4.70 m: Stop one RO unit.
High level 2= 5 m: Stop the second RO unit (both stopped).

2.2 Bond graph model of the cement water treatment process

The bond graph formalism is an universal language able to model the energetic transfers in many fields such as mechanical, electrical, hydraulic and thermodynamic. Accordingly, the bond graph is used to model our described system. Initially, the whole process detailed in the previous section is modelled by a word bond graph represented in Fig. 2. In this scheme, the main parts which compose the real systems are schematized and will be well detailed in the following sections. The model involves two physical domains, namely (1) the mechanical rotation and (2) the hydraulic domain. Based on the experimental parameters which are well identified by using the experimental characterization, the model will be able to correctly define the real behavior.

2.2.1 Tank model

The water treatment process contains three tanks namely, raw water storage, cooling water storage and cooling tower storage. In addition, each tank is defined as the hydraulic capacity derived from the equation in [20] [21]. Then, all these tanks are modeled in bond graph's languages as C-element with (CTank) expressing the hydraulic capacity, (PTank) is the pressure and (QTank) is the water flow stored in the tank , such that:

$$P_{Tank} = \frac{1}{C_{Tank}} \int Q_{Tank} \quad (1)$$

$$C_{Tank} = \frac{A}{\rho g} \quad (2)$$

Where (A) is the section, (g) is the constant of gravity: g = 9.81 m/s² and (ρ) is the density of water.

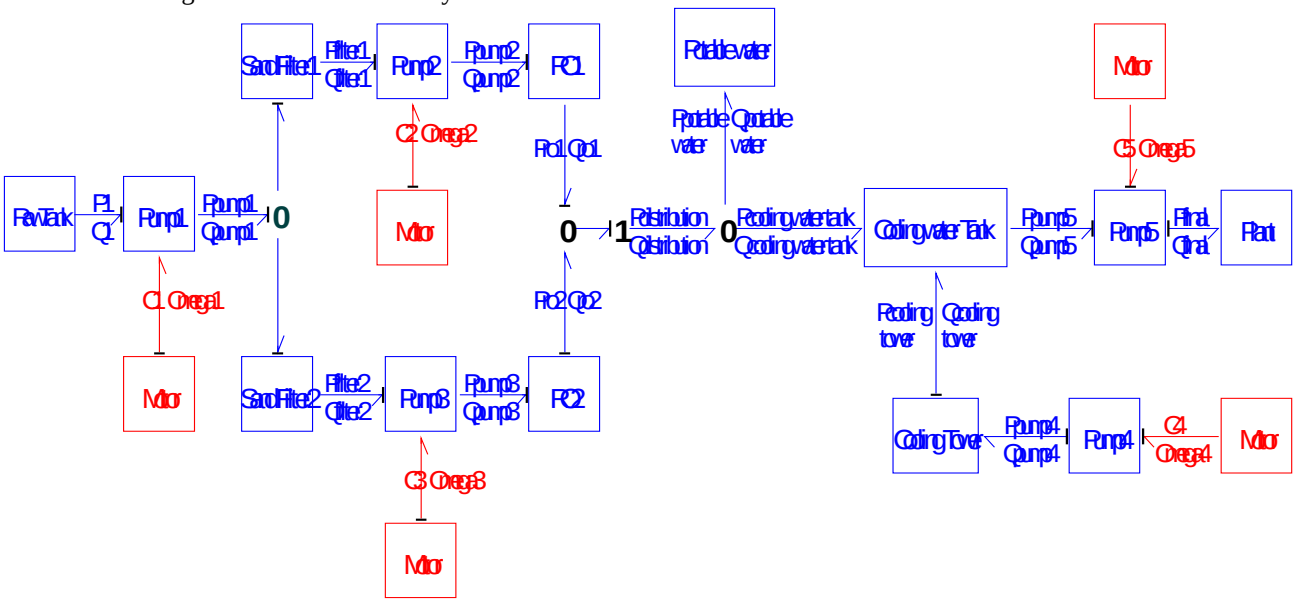

Fig. 2. The Word bond graph's model.

2.2.2 Pump model

The process disposes of five pumps with different parameters as follows:
-Centrifugal Moto-pump of raw water: This pump is Grundfos (NB50-160/167), it permits pumping the raw water to treatment process with a maximum flow of 72 m3/ hour. This one is driven by a three-phase asynchronous motor with 11kW of the rated power.
-Two centrifugal Moto-pump of RO: each pump of the RO unit is Grundfos (CRN45-11), it allows pumping the filtered raw water to the reverse osmosis with a maximum flow product of 36m3/hour. Each pump is driven by a three-phase asynchronous motor with 22kW of the rated power.
- Moto-pump of cooling tower: this centrifugal pump is Grundfos (NK125-500/548), it permits pumping the flow of water from the hot tank to the cooling tower with a maximum flow product of 300m3/hour. This pump is driven by a three-phase Asynchronous Motor with 55 kW of the rated power.
-Moto-pump of distribution: this centrifugal pump is Grundfos (NB50-200/219), it permits pumping the flow coming from the cooling water tank to the plant with a maximum flow product of 350 (m3/hour). It is driven by a three-phase Asynchronous Motor with 22 kW of the rated power. In general, the design of the pump is based on methods using empirical and semi-empirical equations which allow for obtaining the geometry of the hydraulic surfaces insuring a maximum efficiency. In another way, as said in [22], the amount of flow moved by the pump on the total area of its veins, (a), minus the effective loss in the moved flow due to the curvature of veins, (b).
In bond graph language, the mechanical−hydraulic power conversion is modeled in many ways [20]. A non-linear gyrator with (a) and (b) coefficients model is chosen to suit the actual system's behavior [23].

$$P_p = \left(a \times \Omega + b \times Q_p\right) \times \Omega - c \times Q_p^2 \quad (3)$$

$$T_m = (a \times \Omega + b \times Q_p) \times Q_p + (f_m + f_p) \times \Omega \quad (4)$$

Where T_m is the load torque of the motor of pump, (P_p) is the pressure of the fluid, (Q_p) is the pump's flow, (Ω) is the rotation speed of the motor, (a, b) are the pump parameters; and (c) is a parameter presenting the losses in the pump. The losses in the pump's model are identified as follow: where (c) is the hydraulic friction, (J_{pm}= Jp + Jm) is the motor-pump mechanical inertia and (f_{pm} = fp + fm) is the motor-pump mechanical losses [24]. These pump parameters (a, b, c and f_{pm}) are extracted from experiments. The final resulting motor-pump model can be expressed as follows in Fig. 3 after neglecting the equivalent inertia effect (J_{pm}= Jp + Jm) [25].

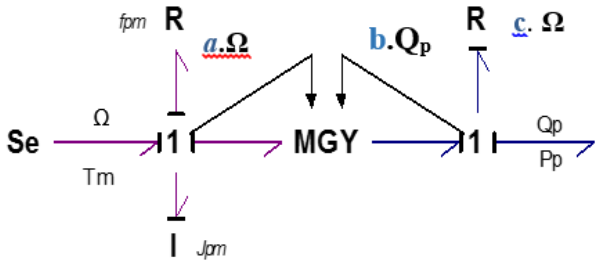

Fig. 3. The pump's Bond Graph Model.

2.2.3 Pipe model

The hydraulic dissipation in the pipes is modeled by an R-element, then the pressure (Ppipe) is computed according to the Bernoulli law [20] [26] as follows:

$$P_{pipe} = R_{pipe} Q_{pipe}^2 \quad (5)$$

Where (P_{pipe}) is the pressure, (Q_{pipe}) is the water flow passing through the pipe and (R_{pipe}) is the debit coefficients.

2.2.4 Reverse osmosis model

The Reverse Osmosis device is the finest filter. By applying an external pressure, which must be superior to the osmosis pressure, the flow direction will be reversed. The mechanism of the RO is summarized in the fact that the feed water enters in the RO membrane under enough pressure to overcome the osmotic pressure. The water's molecules are only allowed to cross through the semi-permeable membrane. The salts and other contaminants are discharged through the concentrate stream which will drain. This phenomenon is demonstrated below in Fig. 4. To summarize, two types of water will be obtained from the water feed. The first one is the permeate which is the good water that comes out of an RO system and has the majority of removed contaminants.

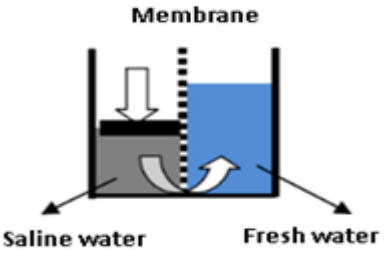

Fig. 4. The outflow water through the RO membrane.

The concentrate, also known as reject or brine, is the second type of water that contains all of the contaminants that are unable to pass through the RO membrane. To model the RO, only the hydraulic domain is taken into account because the consideration of all related domains

such as thermal and chemical domains did not influence the characterization of the current mode and also leads to increase the complexity of model. The RO bond graph model is composed of several elements which will be individually detailed [24] [27] [28]. In reality, the plant is equipped with two identical reverse osmosis RO units. Each RO contains nine vessel pipes and every vessel pipe incorporates three membranes of eight inches. These membranes are EUROWATER series 03-27 which is designed with a flow rate from 5 to 30 m3/hour. The important element in RO is the membrane which is modeled as a C-element corresponding to an hydraulic capacity. To characterize the membrane's permeability, the mechanism of mass transport across the membrane, commonly known as the "solution- diffusion" model, is considered. The solution-diffusion transport equation for the reverse osmosis can be derived as follows:

$$J = L_m \left(\Delta P - \Delta \Pi\right) \quad (10)$$

Where (J) is the water flux through the membrane, (Δp) is the transmembrane pressure difference, (Δπ) is the difference in osmotic pressure between the feed and the permeate and (L_m) is the permeability coefficient of the membrane.

The Osmotic pressure of the feed and permeate solutions play a role in the separation process. In fact, the pressure needed to force a solvent (water), to leave a solution and to oblige permeates to pass through the membrane. For an ideal solution with a complete dissociation of salt ions, the osmotic pressure is defined as:

$$\Pi = iCRT \quad (11)$$

Where (π) is the osmotic pressure, (C) is the salt ion concentration, (R) is the ideal gas constant, (T) is the solution temperature and (i) is the number of the ions in solution. The losses in the RO are also modeled as R-elements. They are subdivided into losses in pipes, also known as a loss of pressure between the input and rejection sides, and a loss at the output of the rejected water through the control valve. The variation in the position of this valve depends on the recovery ratio which causes a variation in the pump's hydraulic load. All these losses are respectively represented in the RO model by (R_{pipe}), (R_{module}) and (R_{valve}) as shown in Fig. 5.

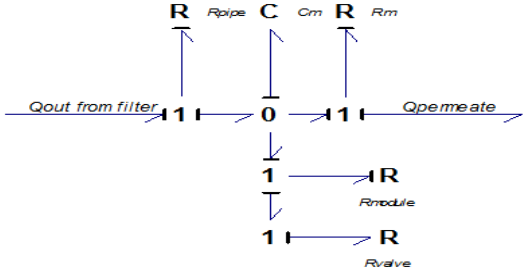

Fig. 5. RO's Bond Graph Model

2.2.5 Cooling tower model

The principle of the cooling tower is briefly described in [29]. As said in [29], this phenomenon consists of the evaporation of the falling water film on the fill packing due to its interaction with the rising air stream which results in the cooling of the water stream as well as the heating and humidification of the outlet air. Due to the complexity of the thermal phenomenon in the cooling tower, only the hydraulic part is studied in this model. Furthermore, the equations of the mass conservation of the two phases which are available in the cooling towers derived two forms as shown in equation (12) and equation (13) below. The first one is the mass conservation for the dry air and the second is the mass conservation for water.

$$\dot{m}_{air,in} = \dot{m}_{air,out} \quad (12)$$

$$\dot{m}_{water,in} + w_{air,in}\,\dot{m}_{air,in} = \dot{m}_{water,out} + w_{air,out}\,\dot{m}_{air,out} \quad (13)$$

With $(\dot{m}_{air,in})$ and $(\dot{m}_{air,out})$ are the mass flow inlet and outlet of air and $(\dot{m}_{water,in})$ and $(\dot{m}_{water,out})$ are the mass flow inlet and outlet of water and (w) is the humidity ratio. The last equations allow approaching the model of the cooling towers. Indeed, the cooling towers are modeled as an R-element which represents the flow of water lost in the vapor cooling tower is seen as a hydraulic capacity.

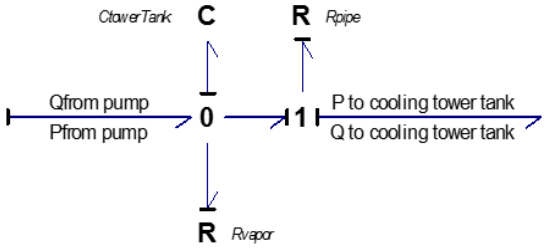

Fig. 6. Cooling Tower's Bond Graph Model.

2.2.6 Hybrid bond graph modeling system

Aim to model the real behavior of the cement water treatment process; the bond graph model must consider the hybrid character of this system. To detail, the cooling water tank level able to give order to start run the both lines of the RO or stop one and let just one line in function. This was described in the section 2. Closely, in this model we just reveal the significant modes which affect directly the functioning of the process. The first mode is defined when the level in cooling water tank reaches about 2.50 m: this level let start the run of the two RO units. Similarly for the second mode, the level is the only responsible on the control of ON and OFF of the osmosis lines. So for a level of 4.70 m, the cooling water

tank let work only one RO unit and stop the second. To highlight this discontinuity in our bond graph model and approach its more to the reality, we refer to the hybrid bond graph and precisely the controlled junction. It behaves as a normal 1- or 0-junction when ON and a source of zero flow or effort (respectively) when OFF [30]. The controlled 1-junction is therefore used to inhibit flow and a controlled 0-junction is used to inhibit effort. The commonly accepted notation for controlled junctions is X1 and X0. In our model, we deal with autonomous switching when the convenient level is reached the junction commutates. So, we browse a logical function for decision which able to determine the suitable level for switching. To recapitulate, the bond graph model of whole process is shown in appendix.

3. Experimental validation of the process

The simulations of the BG model of the cement water treatment process are achieved by the 20-Sim© software, especially adapted for dynamic modeling of multidisciplinary energy systems. Then, we compare these elaborated simulations with the experimental results. In second phase, a series of illustrations is presented that demonstrate the accuracy of the proposed bond graph model. In reality, the Fig. 8 and Fig. 9 show the first mode of the system when the two lines operate together. As said before, the level of cooling water tank determines the operating mode of the treatment process. Consequently, the Fig. 7 and Fig. 10 imply the autonomous character of the switching. Indeed the Fig. 7 demonstrates that the chosen range of level from 2.7 m to 3.06 m is corresponded to the right condition for establishing the first mode which illustrated respectively in the curve of Fig. 8 and Fig. 9. In fact, Fig. 8 show that the real permeate flow of the first osmosis isn't far from the same flow obtained by the hybrid bond graph model. Similarly, the curve drawn in Fig. 9 shows that, despite some errors, simulation results of the second RO in the first mode process model are adequately conform to experimental results. When the level in the cooling water achieves 4.7 m, the system switches to the second mode where only one reverse osmosis is operating. Practically, for the range of level from 4.74 m to 4.92 m which is illustrated in Fig. 10, our model switches as the real process to the second mode. So the curves respectively in Fig. 11 and in Fig. 12 demonstrate well this mode. They explain that the behaviors of the simulated and the experimental permeate flow of the first osmosis in this current mode are conform. By the same way, in the second osmosis, the simulated and experimental permeate flow of this osmosis in this current mode reflect that only one osmosis is ON state.

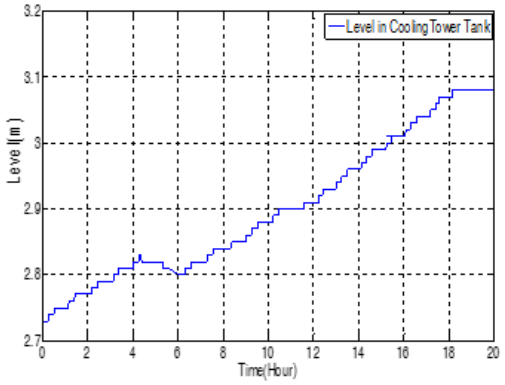

Fig. 7. The cooling water level controlling the first mode.

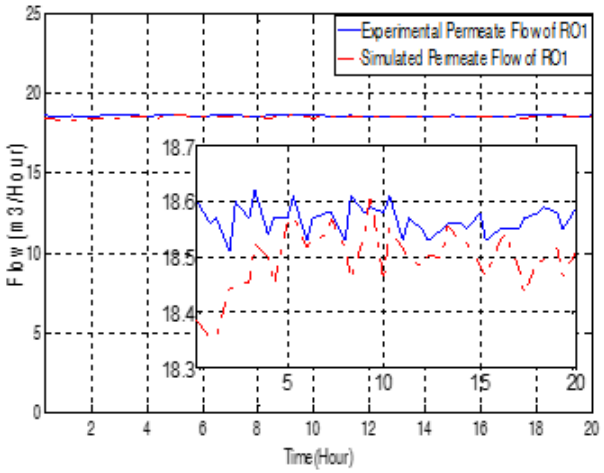

Fig. 8.The behavior of the permeate flow of RO 1 in the first mode.

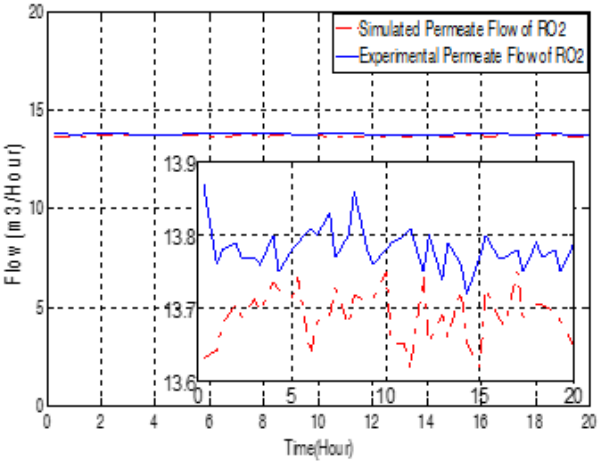

Fig. 9. The behavior of the permeate flow of RO 2 in the first mode.

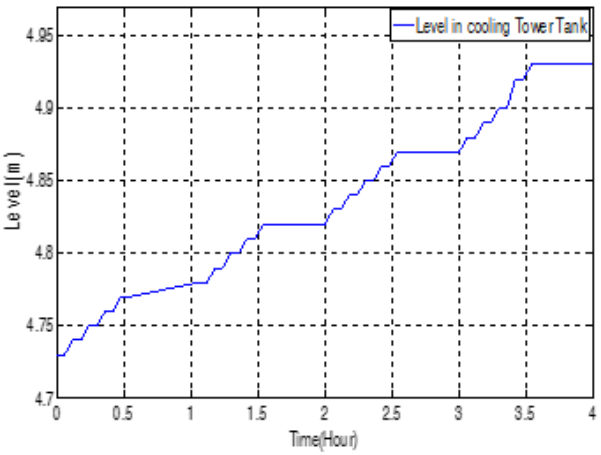

Fig. 10. The cooling water level controlling the second mode.

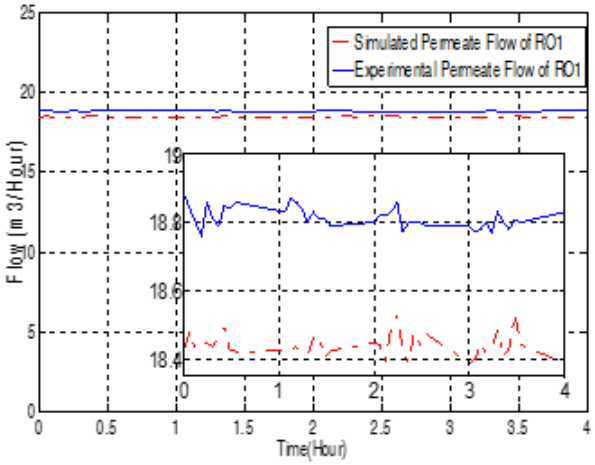

Fig. 11. The behavior of the permeate flow of RO 1 in the second mode.

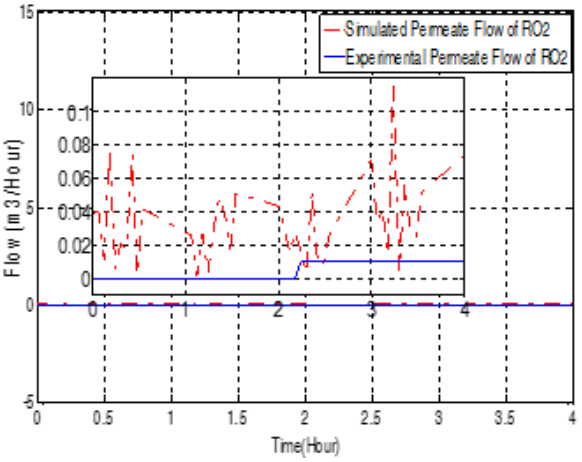

Fig. 12. The behavior of the permeate flow of RO 2 in the second mode

4. Robust hybrid bond graph observer for mode identification and sensor fault detection and localisation

Firstly, we investigate the luenberger bond graph observer in identifying the current mode by evaluating the obtained residuals. A second structure composed by DOS (Dedicated Observer) scheme is used then to detect and locate the sensor faults. Combining these described structures, a new hybrid bond graph observer is constructed as is demonstrated in fig.13 allowing in one way the mode identification of the HDS modelled by switching bond graph and in another way the detection and the localization of the sensor fault of this system.

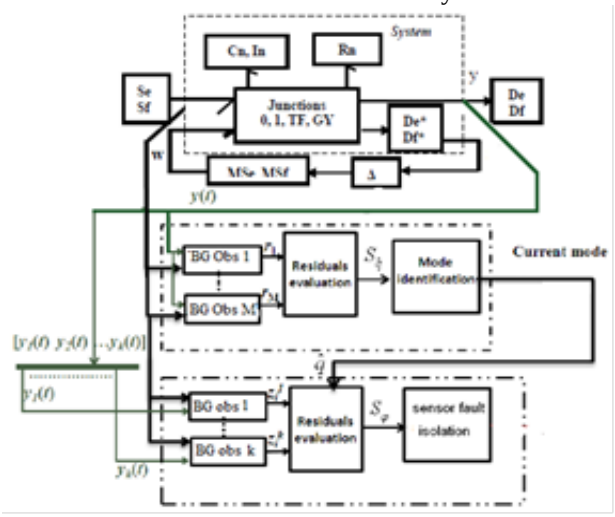

Fig. 13. The hybrid bond graph observer.

4.1 Mode identification procedure in presence of measurement uncertainties and in absence of faults

A new technique focusing on the use of the bond graph observer which is based on the BG-LFT model is presented in this paper aiming to identify the current mode. This latter is investigated in favor of the diagnosis procedure by including the mode identification for the HDS modelled by the switching bond graph. For the real systems the uncertainties and the modeling errors present many problems such as false alarms and non-detections, thus undermining the confidence in the diagnosis system. So, the idea here is to determine a procedure based on the bond graph observer to identify the current mode of the system which takes into account the presence of the measurement uncertainties. Mainly, the identification phase consists of the elaboration of banks of M (number of modes) Luenberger bond graph observers associated to each mode of the system. In fact, each observer receives all

I/O of HDS modes, and then its reconstructed output $\hat{y}(t)$ is compared, at any time, to the measured outputs $y(t)$for generating the residual vectors $r_i(t)$[10]. In order to assess the obtained residuals, a theoretical signature table is elaborated then, it will be compared to the experimental signature table obtained to decide about the current mode. The experimental signature is governed by the following logic of decision as follows:

$$\begin{aligned} Sr_{ij} &= 0 \quad if \quad |r_{ij}| > S_{ij} \\ Sr_{ij} &= 1 \; if \quad |r_{ij}| < S_{ij} \\ Sr_i &= \prod_{j=1}^{k} Sr_{ij} \qquad i = 1 \ldots M \end{aligned} \tag{14}$$

With r_{ij} is the residual error of each mode. S_{ij} is the threshold deduced from the maximum of the uncertain part which is separated from the nominal part of the residuals. $|r_{ij}|$ is the absolute value of the residual. Sr_i is the experimental signature of mode *i*.

In bond graph approach, the thresholds generation is derived from the observer's residuals which are designed in accordance with the BG-LFT model. It consists on decoupling the uncertain part of the residuals from the nominal then generating the threshold of the residuals using the maximum of the uncertain part. In fact the measurement uncertainties in bond graph are previously modeled in [19] in purpose to the diagnosis by analytical redundancy relations (ARRs), by replacing the junction that contains the detector with a sub-model that corresponds to this junction as shown in Fig. 14. The measurement error is represented by a virtual source of flow or effort depending on the nature of the detector.

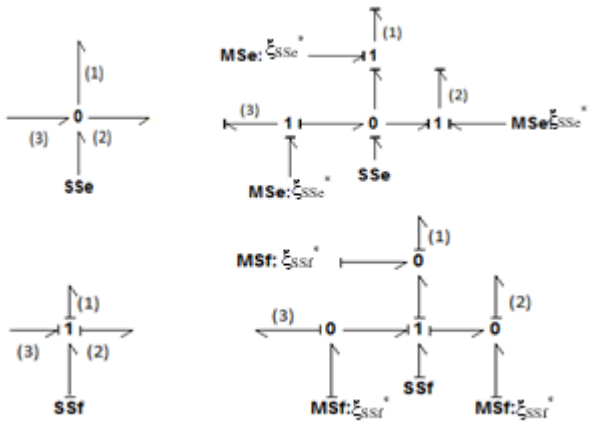

Fig. 14.Mesurement uncertainty Modelling.

4.2 Sensor faults detection and isolation by bond graph observer

The second module of our described hybrid bond graph observer is composed by DOS (Dedicated Observer) scheme. For k sensor faults and for each mode i (i=1... M), the DOS-based bond graph observer scheme is used to generate a residual sensitive to a single sensor fault. The structure of the sensitive j[th] component observer of the output vector is given by the following equation:

$$BG\_OBSF \begin{cases} \dot{\hat{x}}(t) = \begin{pmatrix} \dot{\hat{p}}_I \\ \dot{\hat{q}}_C \end{pmatrix} = A \begin{pmatrix} p_I \\ \hat{q}_C \end{pmatrix} + Bu(t) + L_i^j (y_j(t) - y_j(t)) \\ \hat{y}_j = C \begin{pmatrix} \hat{p}_I \\ \hat{q}_C \end{pmatrix} \\ z_i^j(t) = (y_j(t) - \hat{y}_j(t)) \end{cases}$$

With $\hat{x}$ is the estimate state vector, $\hat{y}$ is the estimate output, u(t) is the input vector, y(t) is the output vector, p and q are the energetic variables of BG modeling (p: momentum, q: displacement), A, B and C are constant matrices with appropriate dimension. L is the observer gain. After determining the gain of each component observer of the output vector by the pole placement method, another procedure of evaluation is applied to evaluate the obtained structured residuals. It is based on comparing the norm structured residual with the threshold "S_{ij}", which is calculated on a T window of length 1s and it is defined as follow:

$$\left\| z_i^j(t) \right\|_{2,T} = \sqrt{\left[\int_{t-T}^{t} z_i^T(t) z_i(t) dt \right]}$$

The decision logic of this comparison is :

$$S_{zi}^j = 1 if \left\| z_i^j(t) \right\|_{2,T} > S_{ij}$$

$$S_{zi}^j = 0 if \left\| z_i^j(t) \right\|_{2,T} < S_{ij}$$

With S^j_{zi} is the experimental signature.

The threshold of detection is calculated as follows:

$$S_{ij} = \sup \left\langle \left\| z_i^j(t) \right\|_{2:T} \Big| \, \phi = 0 \right\rangle$$

5. Application

5.1 System description

In aim to apply the latter procedure and for raisons of simplification, the cement water treatment process described in the previous sections is simplified by considering the two pumps of reverse osmosis which are

fed by the flow of water post filtered of each train as inputs to our simplified system and replacing the cooling towers process by a simple source of flow. The obtained system is demonstrated below in Fig. 15.

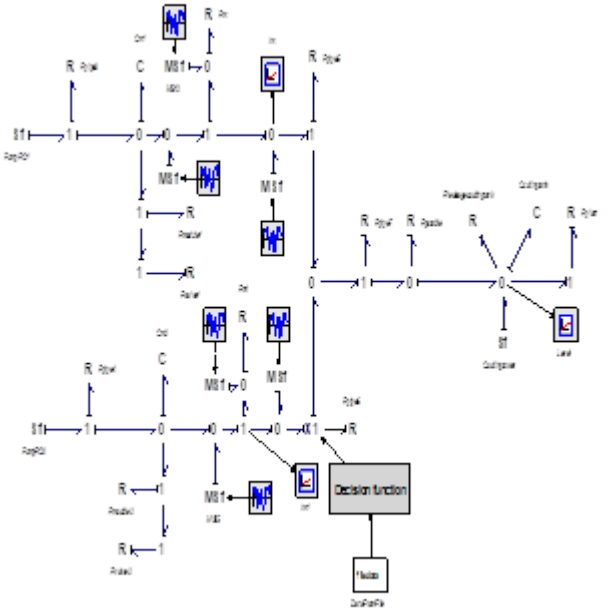

Fig. 15.The simplified cement water treatment process.

5.2 Mode identification in absence of faults

In this system, the banks of two bond graph observers dedicated to identify the current mode are elaborated. Each observer is associated to one mode to estimate the current mode. To determine the observer's gains a pole placement technique is used for each mode. Each observer gain is represented as follows:

$$K_1 = 10^5 * \begin{pmatrix} 1.8588 & 0.0016 & 0 \\ 0.0009 & 0.0245 & 0 \\ 0 & 0 & 0 \end{pmatrix}$$

$$K_2 = \begin{pmatrix} -0.5246 & 0 & 0 \\ 0 & 0 & 0 \\ 0.003 & 0 & 0.0016 \end{pmatrix}$$

As previously mentioned, in the presence of a measurement noise, the computation of the threshold is derived from the observer's residuals. For each mode, the measurement uncertainties are applied to the sensor of flow 1 and flow 2 respectively noted as ξ_{Im} and ξ_{Im1}. We estimate that the sensor of level is noise free (the sensor responsible to differentiate each mode). The threshold can be obtained using the bond graph model directly as in [19] and [27]. We separate the uncertain part of the residuals generated by each bond graph observer from the nominal part.

Then, we get the threshold of the residuals using the maximum of the uncertain part. We extract the thresholds for each mode using equations (15), (16), (17), (18), (19) and (20).

$$\begin{aligned} \mathbf{R}_{11} &= \mathbf{r}_{n11} + \mathbf{d}_{11} \\ \mathbf{r}_{n11} &= -K_{11} * r_{11} - K_{21} * r_{12} - K_{31} * r_{13} \\ |\mathbf{d}_{11}| &= \xi_{Im} \end{aligned} \tag{15}$$

$$\begin{aligned} \mathbf{R}_{12} &= \mathbf{r}_{n12} + \mathbf{d}_{12} \\ \mathbf{r}_{n12} &= -K_{12} * r_{11} - K_{22} * r_{12} - K_{32} * r_{13} \\ |\mathbf{d}_{12}| &= \xi_{Im1} \end{aligned} \tag{16}$$

$$\mathbf{R}_{13} = \mathbf{r}_{n13} + \mathbf{d}_{13}$$

$$\mathbf{r}_{n13} = \frac{(R_{plant} - k_{13})r_{11} + (R_{plant} - k_{23})r_{12} - R_{plant}C_3\frac{dr_{13}}{dt} - r_{13}k_{33}}{1 + \frac{R_{plant}}{R_{potable}} + \frac{R_{plant}}{R_{leakagecooling\ tank}}} \tag{17}$$

$$|\mathbf{d}_{13}| = \frac{R_{plant}(\xi_{Im1} + \xi_{Im})}{1 + \frac{R_{plant}}{R_{potable}} + \frac{R_{plant}}{R_{leakagecooling\ tank}}}$$

$$\begin{aligned} \mathbf{R}_{21} &= \mathbf{r}_{n21} + \mathbf{d}_{21} \\ \mathbf{r}_{n21} &= -K_{11} * r_{21} - K_{31} * r_{23} \\ |\mathbf{d}_{21}| &= \xi_{Im} \end{aligned} \tag{18}$$

$$\mathbf{R}_{22} = 0 \tag{19}$$

$$\mathbf{R}_{23} = \mathbf{r}_{n23} + \mathbf{d}_{23}$$

$$\mathbf{r}_{n23} = \frac{(R_{plant} - K_{13})r_{11} - R_{plant}C_3\frac{dr_{23}}{dt} - r_{23}K_{33}}{1 + \frac{R_{plant}}{R_{potable}} + \frac{R_{plant}}{R_{leakagecooling\ tank}}} \tag{20}$$

$$|\mathbf{d}_{23}| = \frac{R_{plant}(\xi_{Im})}{1 + \frac{R_{plant}}{R_{potable}} + \frac{R_{plant}}{R_{leakagecooling\ tank}}}$$

All output errors are considered to be bounded as follows:

$$|\xi_{Im}| < 0.0054 m^3 / hour$$

$$|\xi_{Im1}| < 0.054 m^3 / hour$$

As a result, it is obvious from Fig. 15 that each component of the vectors of residuals $r_i(t)$ converges towards zero only when the HDS evolves in mode i, otherwise it notably moves away from zero.

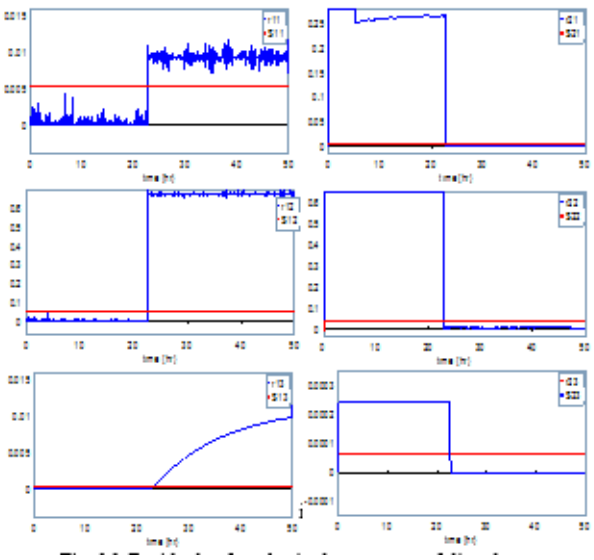

Fig. 16. Residuals of modes in the presence of disturbances (measurement noise) and their corresponding thresholds.

Base on the evaluation procedure of the mode identification, the experimental signature confirms the pertinence of this procedure and shows a concordance with the theoretical signature table as demonstrate in Fig. 17. Table I details the result obtained from the mode identification. Closely, the first mode remains constant until the instant 22.63 hour then the second mode stay until the 50 hour.

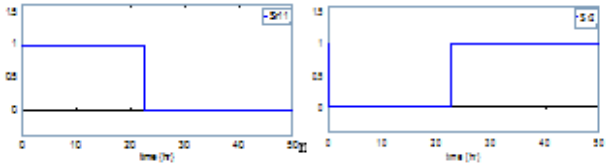

Fig. 17. Modes signatures in the noisy case

TABLE I: Identification of current mode in noisy case

Time interval	Mode Signature		Current Mode
	Sr1	*Sr2*	
0<t<22.63	1	0	Mode1
22.63<t<50	0	1	Mode2

5.3 Mode identification in presence of faults

In addition to the measurement uncertainties, the cement water treatment process occurs a fault in the sensor which computes the permeate flow of the first osmosis (Flow1). This sensor fault φ_1 remains on the time interval of [0s, 5 hour] with an amplitude of 25.92 m^3/hour when the system is in mode 1. To identify the current mode in the faulty case, we repeat the same procedure of the mode identification. The residuals and their corresponding experimental signatures are obtained in the presence of a disturbance and fault as shown in the Fig. 18 and Fig. 19.

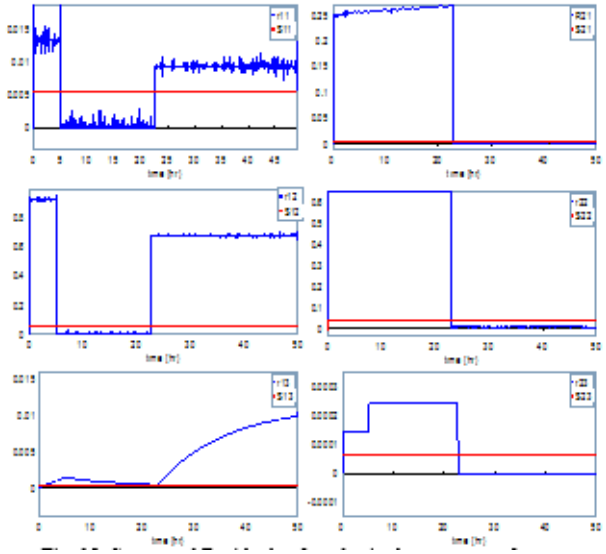

Fig. 18. Structured Residuals of modes in the presence of sensor fault and in noisy case

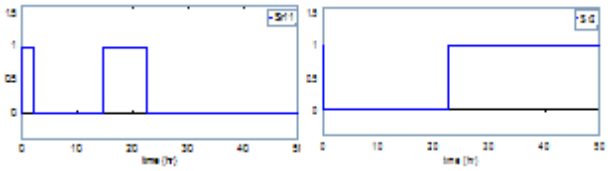

Fig. 19. Modes signatures in the faulty and noisy case

It's obvious that the fault in the sensor of the flow1 has an impact on the obtained residuals especially those in mode 1, as affirmed by the experimental signatures above. But, this result does not prove that the faulty sensor can be isolated. In the next step, we use k bond graph observers which correspond to the identified mode as each of these observers is sensitive to a single output [10]. As stated before in [27], for k sensor faults and for each mode i (i=1... M), a DOS-based bond graph observer scheme is used to generate a residual sensitive to a single sensor fault. In this case, the gain matrices that ensure the convergence of each observer are mentioned below:

$$L_1^1=\begin{pmatrix}9.394\\ -.1955\\ -74.0512\end{pmatrix}, L_1^2=10^4*\begin{pmatrix}-0.0469\\ 0.05\\ -3.2104\end{pmatrix}, L_1^3=10^3*\begin{pmatrix}-7.569\\ 7.5727\\ 0.102\end{pmatrix}$$

$$L_2^1=\begin{pmatrix}0.0011\\ \\ -2.5924\end{pmatrix}, L_2^2=\begin{pmatrix}0\\ 0\\ 0\end{pmatrix}, L_2^3=\begin{pmatrix}-0.1879\\ 0\\ 0.0994\end{pmatrix}$$

Applying now the cited procedure of evaluation based on the norm structured residual, the evaluated residuals and their chosen thresholds are shown in Fig. 20 and Fig. 21 introduces the experimental signatures of the mode for the sensor fault detection.

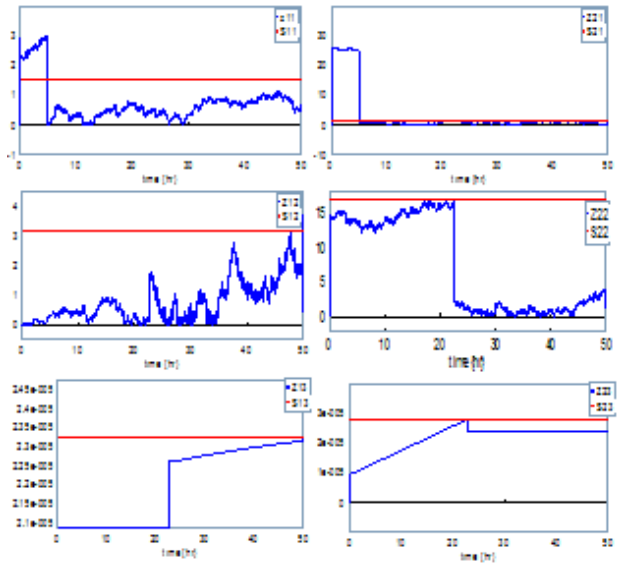

Fig. 20. Norm evolution of the structured residuals and detection thresholds of sensor faults for the two modes.

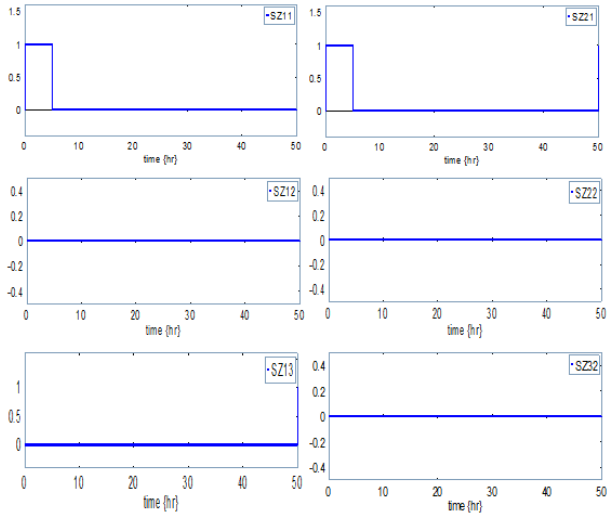

Fig. 21.Structured experimental Signature of residuals for the detection of the sensor faults.

Table II summarizes the results of the identification modes as well as faults detection and isolation. We notice that fault is detected from the 0 s to 5.0002 hour, this time indicating the presence of a sensor fault in output 1 (Sz11=1 and Sz21=1).

TABLE II: Mode identification and fault sensor detection and isolation

Time interval	Mode Signature		Fault Signature		Current Mode
	Sr1	*Sr2*	*Sz11 Sz12*	*Sz21 Sz22*	
0<t<22.63	1	0	10	10	Mode1
22.63<t<50	0	1	00	00	Mode2

6. Conclusion

In this paper, a modeling of cement water process is presented. A model of a real industrial process that takes into consideration many physical fields and presents a hybrid dynamic behavior is developed. To do so, we used the formalism of the hybrid bond graph because it is considered as a suitable tool to model the multidisciplinary process. The experimental and simulation results showed the efficiency of the implemented model using hybrid bond graph formalism. Moreover, the robust fault detection and isolation (R FDI) by hybrid observer technique that is based on BG modeling is applied to the cement water treatment process in purpose to identify the current mode, detect and isolate the sensor fault. This latter approach is divided in two modules. The first one is based on using bank of bond graph observers for each mode in order to generate the residuals system in the presence of the measurement noises in the first place and an added sensor fault in the second. The second developed module is the bank of bond graph observers (DOS) for the isolation of the sensor fault.

References

[1] K.. Medjaher, “Contribution de l’Outil Bond Graph pour la Conception de Systèmes de Supervision des Processus Industriels”, Thèse de doctorat, 2005, USTLille1-ECLille.

[2] G. Dauphin-Tanguy and C. Rombaut, “Why a unique causality in the elementary commutation cell bond graph model of a power electronics converter”, IEEE international conference on systems, man and cybernetics 1, pp.257–263, 1993.

[3] A. Canstelain, “Modelling and analysis of power electronic networks by bond graph”, In Proc. 3rd Int. Conf. Modelling and Simulation of Electrical Machines and Static Converters, IMACS-TCI 90 Nancy, France, 1990, pp. 405-416.

[4] M. Delgado and H. Sira-Ramirez, (1995). “Modelling and Simulation of Switch regulated dc-to-dc power converters of boost type,” in proceeding 1995 IEEE 1st International Conference on Devices Circuits and Systems, Caracas, pp.84-88.

[5] J. F. Broenink, and C. J. Wijbrans, “Describing discontinuities in bond graphs,” in Proc. 1993 Western Simulation Multiconference. Int. Conf. on Bond Graph Modeling ICBGM'93, La Jolla, CA, 1993, pp. 120-125.

[6] A. Nacusse, and S. Junco, "Switchable structured bond: A bond graph device for modeling power coupling/decoupling of physical systems," Journal of computational science (2013).
[7] A. C. Umarikarand L. Umanand, "Modelling of switching systems in bond graphs using the concept of switched power junctions," J. Franklin Institute, vol. 342, iss.2 pp. 131-147, Mar. 2005.
[8] P. J. Gawthrop, "Hybrid Bond Graphs using Switched I and C Components," Centre for Systems and Control, University of Glasgow, Glasgow, UK. CSC Report 97005, 1997.
[9] P. J. Mosterman, and G. Biswas, "Modeling Discontinuous Behavior with Hybrid Bond Graphs," In 9th Int. Workshop on Qualitative Reasoning about Physical Systems, Amsterdam, Netherlands, 1995, pp. 139-147.
[10] A. Takrouni, "Robust Diagnosis for Hybrid Dynamical Systems," International Journal of Engineering and Innovative Technology (IJEIT) Volume 3, Issue 9, March 2014.
[11] D. Belkhiat, "Diagnostic d'une classe de systèmes linéaires à commutations: Approche à base d'observateurs robustes," Thesis, University of Reims, December (2012).
[12] F. Hamdi, "Contribution à la Synthèse d'Observateurs pour les Systems Hybrides," Thesis, University of Batna Faculty of Science of engineering electronic department, 13 Jul. 2010.
[13] V. Cocquempot, M. Staroswiecki and T. EL Mezyani, "Switching time estimation and fault detection for hybrid systems using structured parity residuals," 5th IFAC Symposium on Fault Detection, Supervision and Safety of technical Processes, Washington DC, USA, pp. 681-686,(2003).
[14] A. Hakem, K. M. Pekpe and V. Cocquempot "Parameter-free method for switching time estimation and current mode recognition," Conference on Control and Fault Tolerant Systems, Nice, France.
[15] W. Borutzky, "Bond graph model-based system mode identification and mode-dependent fault thresholds for hybrid systems," Mathematical and Computer Modelling of Dynamical Systems: Methods, Tools and Applications in Engineering and Related Sciences, (2014).
[16] S.A. Arogeti, D. Wang, C.B. Low and J.J. Zhang, "Energy based mode tracking of hybrid systems," Proceedings of the 17th World Congress, The International Federation of Automatic Control. Seoul, 2008, pp. 12813–12818.
[17] S.A. Arogeti, D. Wang, and C.B. Low, "Mode identification of hybrid systems in the presence of fault," IEEE Transactions on Industrial Electronics, 57(4):1452-1467, 2010.
[18] M.A. Djeziri, R. Merzouki, B. Ould Bouamama, and G. Dauphin-Tanguy, "Robust fault diagnosis by using bond graph approach," IEEE/ASME Trans. Mech. 12 (6) (2007 December), pp. 599–611.
[19] Y. Touati, R. Merzouki, and B. Ould Bouamama, "Fault detection and isolation in presence of input and output uncertainties using bond graph approach," in Proceedings of the 5th International Conference on Integrated Modeling and Analysis in Applied Control and Automation (IMAACA 2011), A. Bruzzone, G. Dauphin-Tanguy, S. Junco, M.A. Piera M.A., eds., DIPTEM, Genoa, 2011, pp. 221–227.
[20] B. Ould Bouamama, and A.K. Samantaray, "Model-based Process Supervision. A Bond Graph Approach," Springer Verlag, published on 2008, Berlin, 2006.
[21] W. Brotusky, "Bond graph methodology – development and analysis of multidisciplinay dynamic system models," London: Springer, 2010.
[22] P. J. Mosterman, "Hybrid dynamic system: A hybrid bond graph modeling paradigm and its application in diagnosis," Doctoral Thesis, Nashville Tennessee, 1997.
[23] M. Turki, J. Belhadj and X. Roboam, "Control strategy of an autonomous desalination unit fed by PV-Wind hybrid system without battery storage," Journal of Electrical Systems (JES), Volume 4, Issue 2, Juin 2008.
[24] I. Ben Ali, M. Turki, J. Belhadj and X. Roboam, "Systemic design of a reverse osmosis desalination process powered by hybrid energy system," Electrical Sciences and Technologies in Maghreb (CISTEM), 2014 International Conference on, on page(s): 1-6.
[25] J.F. Gülich, "Centrifugal Pumps," 964. Springer, Verlag Berlin Heidelberg, New York ,(2008).
[26] E. Aridhi, M. Abbes and A. Mami, "Pseudo bond graph model of a thermohydraulic system," International Conference on Modeling, Simulation and Applied Optimization, Apr 2013, Tunis, Tunisia.
[27] A. Sellami, "Supervision des systèmes dynamiques Modélisés par approche bond de graph diagnostic et reconfiguration," Thèse de doctorat, école national des ingénieurs de Tunis, 2014.
[28] G. Biswas, E.J. Manders, J. Ramirez, N. Mahadevan and S. Abdelwahed, "Online Model-based Diagnosis to support autonomous operation of an Advanced Life Support System," Habitat: Int. J. Human Support Res., pp. 21-38, 2004.
[29] V.D. Papaefthimiou, T.C. Zannis and E.D. Rogdakis, "Thermodynamic study of wet cooling tower performance," International Journal of Energy Research 30 (2006), pp. 411-426.
[30] R. Margetts, "Construction and Analysis of Causally Dynamic Hybrid Bond Graphs," Proc. IMechE Part I - J. Syst. and Control Eng., vol. 227, iss. 3 pp. 329-346, Mar. 2013.

Eya Fathallah received engineering's degree in electrical from Engineering School of Monastir, Tunisia in 2010. She is currently working toward the Ph.D degree in Laboratory on Analyse, Conception and Control of Systems (ACS), National Engineering School of Tunis (ENIT), University Tunis El Manar.

Nadia Zanzouri received the S.M and Ph.D degrees in electrical engineering from Engineering School of Tunisia (ENIT) in 1999 and 2003 respectively. She is currently an associate professor at Preparatory Engineering Institute of Tunisia and researcher at Laboratory ACS of ENIT. Her research interests include Bond Graph modelling, Robust Fault Detection and Isolation (FDI) and Fault Tolerant Control (FTC) for Dynamical Systems and Hybrid Systems

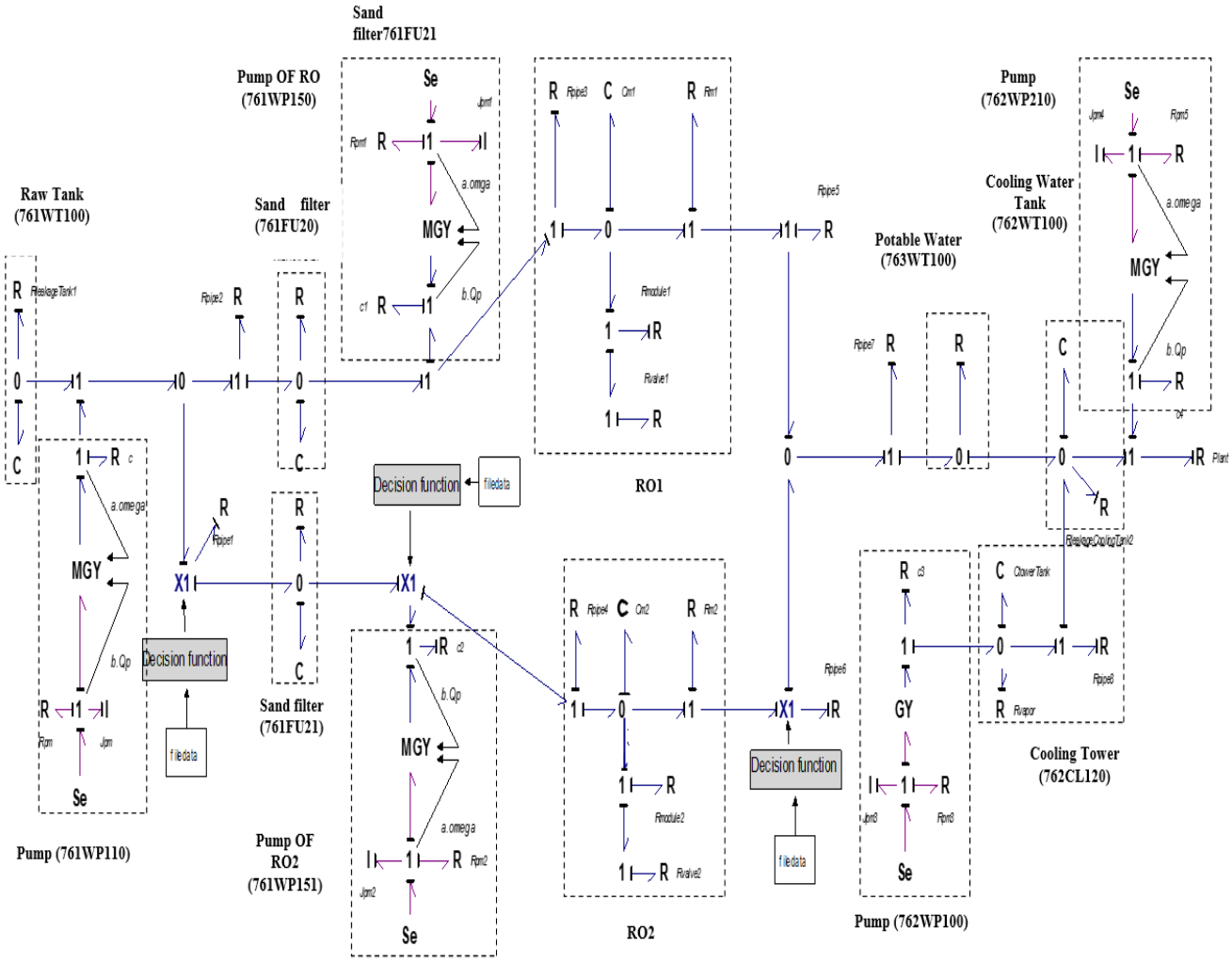

Fig. 22. The hybrid bond graph model of the cement water treatment process